JAERI-M--91-208

JP9207347

JAERI - M
91-208

EXPERIMENTAL EVIDENCE OF OFF-DIAGONAL TRANSPORT TERM AND THE DISCREPANCY BETWEEN ENERGY PARTICLE BALANCE AND PERTURBATION ANALYSES

December 1991

Keisuke NAGASHIMA and Takeshi FUKUDA

日 本 原 子 力 研 究 所
Japan Atomic Energy Research Institute

JAERI-M レポートは、日本原子力研究所が不定期に公刊している研究報告書です。

入手の問合わせは、日本原子力研究所技術情報部情報資料課（〒319-11 茨城県那珂郡東海村）あてにお申し越しください。なお、このほかに財団法人原子力弘済会資料センター（〒319-11 茨城県那珂郡東海村日本原子力研究所内）で複写による実費頒布をおこなっております。

JAERI-M reports are issued irregularly.

Inquiries about availability of the reports should be addressed to Information Division, Department of Technical Information, Japan Atomic Energy Research Institute, Tokai-mura, Naka-gun, Ibaraki-ken 319-11, Japan.

Japan Atomic Energy Research Institute, 1991

編集兼発行　日本原子力研究所
印　　刷　㈱原子力資料サービス

JAERI-M 91-208

Experimental Evidence of Off-diagonal Transport Term and the Discrepancy Between Energy/Particle Balance and Perturbation Analyses

Keisuke NAGASHIMA and Takeshi FUKUDA

Department of Fusion Plasma Research
Naka Fusion Research Establishment
Japan Atomic Energy Research Institute
Naka-machi, Naka-gun, Ibaraki-ken

(Received November 12, 1991)

Evidence of temperature gradient driven particle flux was observed from the sawtooth induced density propagation phenomenon in JT-60. This off-diagonal particle flux was confirmed using the numerical calculation of measured chord integrated electron density. It was shown that the discrepancies between thermal and particle diffusivities estimated from the perturbation method and energy/particle balance analysis can be explained by considering the flux equations with off-diagonal transport terms. These flux equations were compared with the E×B convective fluxes in an electro-static drift wave instability and it was found that the E×B fluxes are consistent with several experimental observations.

Keyword: JT-60, Off-diagonal Transport, Perturbation Method, Density Pulse Propagation, E×B Convective Flux

JAERI-M 91-208

非対角輸送項の実験的観測及びエネルギー・粒子バランスと摂動解析の不一致について

日本原子力研究所那珂研究所炉心プラズマ研究部
永島　圭介・福田　武司

（１９９１年11月12日受理）

ＪＴ－60において，鋸歯状波による密度伝搬現象から，温度勾配による粒子束の存在が観測された。この非対角粒子束は，測定された線積分電子密度を数値計算することにより確認された。更に，摂動法とエネルギー・粒子バランスの解析により得られた熱及び粒子の拡散係数の不一致は，非対角項を含めた粒子束方程式を考慮することにより説明できることが分かった。こうした粒子束方程式と，静電的なドリフト波不安定性におけるＥ×Ｂ粒子束とを比較することにより、Ｅ×Ｂ粒子束が，いくつかの実験結果と一致することが分かった。

那珂研究所：〒311－01　茨城県那珂郡那珂町大字向山801－1

Contents

目　　次

I. INTRODUCTION

In fusion research, energy and particle transport phenomena have been one of the most important subjects. However, they are not understood completely and have been denominated as an anomalous transport. In general, transport phenomena have been investigated using two different methods. One is an examination of energy and particle balances in a steady state and the other is a time-dependent analysis of the several plasma parameters or an analysis of dynamic response to some perturbations. The perturbation method was firstly applied to the sawtooth induced heat pulse propagation successfully by Soler and Callen[1] and the estimated electron thermal diffusivity χ_e was consistent with that from the power balance analysis. In ISX-B tokamak[2] it was found that the estimated χ_e from the heat pulse propagation increases with the heating power, as do the values obtained from the power balance analysis. However, recent investigations in large tokamaks such as TFTR[3] and JET[4] indicated that the values estimated from these two methods were not consistent with each other ; the values from the heat pulse propagations were larger than those from the power balance analysis by a factor of 2 to 10. This discrepancy was found in the modulated ECH heating experiment in Doublet-III[5]. The similar result was found with respect to the particle transport, which is that the particle diffusivity D estimated from the sawtooth induced density pulse propagation was larger by several factors than that obtained from the steady state analysis in TEXT[6]. In several tokamaks, χ_e and D were measured simultaneously with the perturbation methods using sawtooth oscillations or pellet injections, and the importance of coupling between the heat and particle fluxes was indicated. However, the experimental results from several machines show that the ratio of χ_e/D is scattered in the range from 1 (in TEXT[7]) to about 7 (in JET[8]).

Up to now, we have not obtained a systematic explanation with respect to these experimental discrepancies. Several theoretical investigations have been devoted to this problem[9-11] and the importance of off-diagonal transport terms was pointed out. In this article we study the relations of thermal and particle diffusivities between the perturbation method and energy/particle balance analysis. We discuss the possibility to explain the complicated experimental observations using the flux equations with off-diagonal transport terms. Firstly, the theoretical formulations including the off-diagonal transport terms are presented, and the relations between the

perturbation method and energy/particle balance analysis are discussed in Sec.II. Next, experimental evidence of off-diagonal particle flux in JT-60 is shown and it is confirmed by the numerical calculation in Sec.III. In Sec.IV, the obtained experimental results are compared with the ExB convective fluxes using the quasi-linear transport formulation. Lastly, a brief conclusion is presented in Sec.V.

II. DISCREPANCY BETWEEN ENERGY/PARTICLE BALANCE ANALYSIS AND PERTURBATION METHOD

Here, we consider the relation between energy/particle balance analysis and perturbation method using the flux equations with off-diagonal transport terms. The particle and heat diffusion equations are

$$\frac{\partial n}{\partial t} = -\frac{1}{r}\frac{\partial}{\partial r}(r\Gamma) + S \tag{1}$$

$$\frac{3}{2}\frac{\partial nT}{\partial t} = -\frac{1}{r}\frac{\partial}{\partial r}(rq) + P \tag{2}$$

where n, T, S and P represent density, temperature, particle source and heat source, respectively. We assume that particle and heat fluxes are written with additions of off-diagonal transport terms as

$$\Gamma = -D\frac{\partial n}{\partial r} - \alpha\frac{\partial T}{\partial r} \tag{3}$$

$$q = -n\chi\frac{\partial T}{\partial r} - n\beta\frac{\partial n}{\partial r} + \frac{5}{2}T\Gamma \tag{4}$$

where D, χ, α and β represent particle diffusivity, thermal diffusivity and off-diagonal transport coefficients, respectively. Here, it should be noted that the experimentally observed inward particle flux corresponds to the off-diagonal flux term due to temperature gradient, instead of the normal particle flow term.

Using the transformations of $n=n_0+\tilde{n}$ and $T=T_0+\tilde{T}$ (where subscripts of

zero and tilde represent equilibrium and perturbing terms), the perturbing parts of n and T can be written from Eqs.(1) and (2) as

$$\frac{\partial \tilde{n}}{\partial t} = D\frac{\partial^2 \tilde{n}}{\partial r^2} + D\left(\frac{1}{r} + \frac{1}{L_D}\right)\frac{\partial \tilde{n}}{\partial r} + \alpha\frac{\partial^2 \tilde{T}}{\partial r^2} + \alpha\left(\frac{1}{r} + \frac{1}{L_\alpha}\right)\frac{\partial \tilde{T}}{\partial r} + \tilde{S} \tag{5}$$

$$\begin{aligned}\frac{3}{2}\frac{\partial \tilde{T}}{\partial t} = &\left(\chi + \alpha\frac{T}{n}\right)\frac{\partial^2 \tilde{T}}{\partial r^2} \\ &+ \left\{\chi\left(\frac{1}{r} + \frac{1}{L_\chi} + \frac{1}{L_n}\right) + \alpha\frac{T}{n}\left(\frac{1}{r} + \frac{1}{L_\alpha} + \frac{5}{2}\frac{1}{L_T}\right) + \frac{5}{2}D\left(\frac{1}{L_n} + \frac{\alpha}{D}\frac{T}{n}\frac{1}{L_T}\right)\right\}\frac{\partial \tilde{T}}{\partial r} \\ &+ \left(D\frac{T}{n} + \beta\right)\frac{\partial^2 \tilde{n}}{\partial r^2} \\ &+ \left\{D\frac{T}{n}\left(\frac{1}{r} + \frac{1}{L_D} + \frac{5}{2}\frac{1}{L_T}\right) + \beta\left(\frac{1}{r} + \frac{1}{L_\beta} + \frac{1}{L_n}\right) + \chi\frac{T}{n}\left(\frac{1}{L_T} + \frac{\beta}{\chi}\frac{n}{T}\frac{1}{L_n}\right)\right\}\frac{\partial \tilde{n}}{\partial r} \\ &+ A\frac{\tilde{T}}{n} + B\frac{\tilde{n}}{n} - \frac{3}{2}\frac{T}{n}\tilde{S} + \frac{\tilde{P}}{n}\end{aligned} \tag{6}$$

where L_n and L_T are scale lengths of density and temperature, and L_D, L_χ, L_α, L_β are scale lengths of each transport coefficients, respectively. $\tilde{S}$ and $\tilde{P}$ are the perturbing terms of particle and heat sources. Coefficients of A and B represent the terms proportional to $\tilde{T}$ and $\tilde{n}$. It is assumed that these terms are negligible, because our attention is put on only the cases that the perturbing quantities are small compared with the equilibrium values and the initial perturbations are localized. These cases correspond to the assumptions of $\tilde{T}/T_0 << 1$, $\tilde{n}/n_0 << 1$ and $\partial\tilde{T}/\partial r >> \tilde{T}$, $\partial\tilde{n}/\partial r >> \tilde{n}$. Moreover, we assume that the perturbing terms of particle and heat sources are negligible.

In the case of $\tilde{T}/T >> \tilde{n}/n$, which is satisfied in the sawtooth induced perturbations found in the several tokamaks[8,12], Eq.(6) is highly simplified as

$$\frac{3}{2}n\frac{\partial \tilde{T}}{\partial t} \approx \frac{1}{r}\frac{\partial}{\partial r}\left\{rn\left(\chi + \alpha\frac{T}{n}\right)\frac{\partial \tilde{T}}{\partial r}\right\} \tag{7}$$

In a strict description, Eq.(7) is correct only in the case of $\partial^2 T/\partial r^2 >> \partial T/\partial r$ or $\chi >> D$, $\alpha(T/n)$. In the sawtooth induced perturbations, the former relation is

satisfied in a region far from the initially perturbed central region, and the latter relation are observed experimentally in several large tokamaks[8,12]. Therefore, it may be considered that Eq.(7) is a reasonable approximation for the sawtooth induced heat pulse propagation analysis.

In the perturbation analysis, it was pointed out that the non-linear dependence of transport coefficients ($D=D(n, \nabla n, T, \nabla T)$, $\chi=\chi(n, \nabla n, T, \nabla T)$, etc) is important[10]. The non-linear dependence on n, ∇n, T and ∇T produce the additional terms proportional to $\partial\tilde{n}/\partial r$, $\partial\tilde{n}^2/\partial^2 r$, $\partial\tilde{T}/\partial r$ and $\partial\tilde{T}^2/\partial^2 r$ in Eqs.(5) and (6). Therefore, the dependence on ∇n and ∇T produces a significant modification in heat/particle pulse propagation. However, it seems that the strong non-linear dependence is contradictory to the pellet injected density perturbation experiments[8,12]. In these experiments, the induced density perturbations were comparable to the equilibrium values and the induced density gradients became larger than those of the equilibriums by a several factor. Therefore, it is inferred that the diffusivity measured from the perturbation method becomes large if particle diffusivity has a strong non-linear dependence. However, the measured particle diffusivities were almost same to the values obtained from the sawtooth induced perturbations, and this experimental results indicate that the non-linear dependence of particle diffusivity is weak. In our analysis this non-linear dependence is not considered, because our interest is to examine the effect of off-diagonal transport terms and the possibility to explain the experimental observations using these terms.

In an equilibrium state, particle and heat fluxes are written from Eqs.(1) to (4),

$$-D\frac{\partial n}{\partial r} - \alpha\frac{\partial T}{\partial r} = \frac{1}{r}\int rS\,dr \tag{8}$$

$$-n\chi\frac{\partial T}{\partial r} - n\beta\frac{\partial n}{\partial r} + \frac{5}{2}T\Gamma = \frac{1}{r}\int rP\,dr \tag{9}$$

For the comparison of transport coefficients, these equations are rewritten as

$$-\left(D + \eta\frac{T}{n}\alpha\right)\frac{\partial n}{\partial r} = \frac{1}{r}\int rS\,dr \tag{10}$$

$$- n\left(\chi - \frac{\alpha\beta}{D}\right)\frac{\partial T}{\partial r} = \frac{1}{r}\int rPdr - \left(\frac{\beta}{D}n + \frac{5}{2}T\right)\frac{1}{r}\int rSdr \qquad (11)$$

where η is defined as $\eta \equiv L_n/L_T$.

Using Eqs.(5), (7), (10) and (11), transport coefficients inferred from the perturbation method (represented by a subscript of PM) and the equilibrium particle and power balance analysis (represented by a subscript of PB) are

$$D_{PB} = D + \eta(T/n)\alpha \qquad (12)$$

D_{PM}= complicated dependence on D, χ, α and β

$$\chi_{PB} \approx \chi - (\alpha/D)\beta \qquad (13)$$

$$\chi_{PM} \approx \chi + (T/n)\alpha \qquad (\text{for } \tilde{T}/T >> \tilde{n}/n). \qquad (14)$$

In the derivation of Eq.(13), the second term of right hand side in Eq.(11) was neglected. It is found that the ratio of D_{PM} and D_{PB} is complicated depending on D, χ, α, β and the initial perturbed values of $\tilde{n}/n_0$, $\tilde{T}/T_0$.

As mentioned earlier, the several experimental results show that the values of χ estimated from the perturbation method are larger than those from the power balance analysis. Here, we define the ratio of these two values as

$$R \equiv \frac{\chi_{PM}}{\chi_{PB}} \approx \frac{\chi + (T/n)\alpha}{\chi - (\alpha/D)\beta} = \frac{1 + (T/n)(\alpha/\chi)}{1 - (\alpha/D)(\beta/\chi)} \qquad (15)$$

For a high temperature plasma, it is considered that particle source is negligible except in a peripheral region. Therefore, $\Gamma \approx 0$ and $\alpha \approx -(n/T)(L_T/L_n)D$. Substituting this relation into Eq.(15), we obtain $R=(1-D/\eta\chi)/(1+n\beta/T\eta\chi)$. This expression shows that if R>1, the relation of $0>-(T/n)D>\beta>-(T/n)\eta\chi$ should be satisfied. The significance of this relation is discussed in Sec.IV.

III. EXPERIMENTAL EVIDENCE OF OFF-DIAGONAL TRANSPORT TERM

From the above mentioned discussion, it seems that the model including off-diagonal flux terms may be one possible candidate explaining the

experimental discrepancies between D_{PB} and D_{PM} or χ_{PB} and χ_{PM}. Here, we show the experimental evidence of off-diagonal transport term (particle flux due to temperature gradient) in JT-60. (The same experimental phenomenon could be observed in JET [13].)

In Fig.1, we show a typical waveform of the density pulse propagation due to the internal disruption, which is a chord integrated electron density measured from the FIR interferometer viewing vertically at r=0.51 m (r/a_p=0.57, a_p is plasma minor radius). To improve the signal to noise ratio, the data was averaged over five sawtooth oscillations in a steady state phase and plotted with 1 msec sampling. The time is set to be t=0.0 sec at the internal disruption. The discharge conditions are major and minor radii of 3.03 and 0.90 m, plasma current I_p=2.7 MA, toroidal magnetic field B_T=4.5 T, surface safety factor q=2.5, chord averaged electron density $\bar{n}_e=5.0\times10^{19}$ m^{-3}, neutral beam heating power P_{NBI}=10.9 MW and limiter configurated circular plasma with hydrogen working gas. In the figure, the abrupt jump-up of density can be seen at t=0.0 sec and subsequently a small density decrease can be seen. A few msec later, a gradual increase can be seen until the density pulse becomes peak at about t=50 msec. Firstly, we explain that the abrupt jump-up is accounted by the initial perturbation due to the internal disruption. The sawtooth inversion radius, which was measured from the soft x-ray emission profile, was about 0.35 m and the mixing radius was estimated to be about 0.49-0.50 m (the mixing radius was determined from the particle/energy conservations between the inside and outside region of inversion radius, and the density and temperature profiles just after the internal disruption were assumed to be flat inside the mixing radius). The effective beam radius of FIR is about 3 cm. Therefore, it should be considered that the initial density perturbation inside the mixing radius was observed as the abrupt jump-up of measured density. Secondly, we consider that a small density decrease after the jump-up is due to the effect of off-diagonal flux term of temperature gradient in Eq.(5). The concave shaped period (t=0-10 msec) of measured density in Fig.1 corresponds to the time of peaking of temperature perturbation in the region where the density perturbation was measured. Lastly, the continuous increase after the small decrease can be considered to be the normal density pulse propagation.

It could be considered that there are two other possibilities for the measured density decrease. One is due to the displacement of plasma column in a horizontal direction according to the internal disruption.

However, in JT-60, FIR interferometers are arranged with vertical viewing chords at the symmetrical positions of r=±0.51 m, and the same density decreases were measured from the both measurement chords. Therefore, it could not be considered that the plasma displacement is the reason. The other possibility is due to the effect from chord integration of perturbing density. In JT-60, it is difficult to obtain local density using Abel inversion technique, because there are only three chords of FIR interferometer (r= -0.51, 0, +0.51 m). To examine the chord integral effect, we calculated the time evolution of chord integrated electron density from Eq.(5) eliminating the off-diagonal term and using the measured plasma parameters. In the calculation, the effect of finite beam radius of FIR was included. The calculated result is shown in Fig.2 and we can see no density decrease as observed in Fig.1.

To confirm that the measured density decrease is due to the off-diagonal term (temperature driven particle flux), we calculated the time evolution of chord integrated electron density from Eqs.(5) and (6) including the off-diagonal terms and it is shown in Fig.3. Clear density decrease as seen in Fig.1 can be found and the total waveforms are very similar to each other. In the calculation, all transport coefficients were assumed to be constant in space and time. The measured temperature and density profiles of $T_0(r)=4.0(1-r^2)^{1.5}$ keV, $n_0(r)=5.0(1-r^2)^{0.5}$ $\times 10^{19}$ m^{-3} were used, and the initial perturbation profiles were determined as the density and temperature profiles just after the internal disruption become flat in the mixing radius. The transport coefficients of off-diagonal terms were determined using the relations of $-\alpha \approx (n/T)(L_T/L_n)D$ and $\beta \approx (T/n)^2\alpha$. The latter relation was inferred from Onsager relation. If it is set to be $-\alpha < (n/T)(L_T/L_n)D$, the calculated density decrease (concave shaped period) becomes smaller than the measured value. Therefore, we conclude that the transport coefficient of off-diagonal particle flux has an opposite sign against that of diagonal term, and the absolute value is comparable to that of diagonal term. (However, the calculated waveform is sensitive to not only D and α but also the perturbation levels of density and temperature and, moreover, χ and β. Therefore, the values of D and α used in the calculation are not so confirmed.)

As discussed above, the evidence of off-diagonal particle flux was confirmed and it may explain the experimentally observed inward particle flow. On the other hand, with respect to the heat flux, the heat pinch model[14] was proposed as an experimental explanation of energy

confinement and, maybe, as an explanation of the discrepancy between χ_{PB} and χ_{PM}. Therefore, the confirmation of the off-diagonal term of heat flux is attractive from the experimental viewpoint. But unfortunately, up to now, we have not observed the obvious effect of off-diagonal heat flux term. It seems that it is difficult to observe the effect of off-diagonal heat flux due to the density gradient, because any density perturbations produce the temperature perturbation. Moreover, in practical experimental conditions, the effect of electron-ion energy equipartition becomes remarkable and distorts the waveform of temperature perturbation.

IV. COMPARISON WITH ExB CONVECTIVE FLUXES

If we consider ExB convective fluxes (particle and heat fluxes), it seems to be natural consequence that the each flux consists of the terms with density and temperature gradients. Therefore, in this section, we estimate the transport coefficients of ExB convective fluxes due to the electro-static drift wave instability and compare them with the experimental observations.

Using a quasi-linear transport formulation[15,16], particle and heat fluxes are

$$\Gamma = \left\langle \int dv \; v_r^* f \right\rangle \equiv \langle \Gamma_k \rangle \tag{16}$$

$$Q = \left\langle \int dv \; \frac{1}{2} m v^2 \; v_r^* f \right\rangle \equiv \langle Q_k \rangle \tag{17}$$

where angular bracket represents an ensemble average with respect to wave number k, and Γ_k and Q_k are the k-components of particle and heat fluxes. v_r is a radial component of ExB drift velocity and it is given by $v_r \simeq -i(k_\theta/B)\phi$ approximately. An asterisk represents a complex conjugate. f represents a fluctuating part of distribution function and it is divided into two parts, adiabatic and non-adiabatic parts, as $f=-(q/T)F\phi+h$, where q, F, ϕ and h represent electric charge, maxwellian distribution function, electro-static potential and non-adiabatic part, respectively. The normalization with $h=(q/T)n\phi\hat{h}$ yields

$$\Gamma_k = - n \left(\frac{T}{qB}\right)\left(\frac{q\phi}{T}\right)^2 k_\theta \cdot I\,m \int dv\ \hat{h} \tag{18}$$

$$Q_k = - n \left(\frac{T}{qB}\right)\left(\frac{q\phi}{T}\right)^2 k_\theta T \cdot I\,m \int dv\ \frac{mv^2}{2T}\hat{h} \tag{19}$$

where Im represents an imaginary part. We define the normalized fluxes by

$$\hat{\Gamma} = Im \int dv\ \hat{h} \tag{20}$$

$$\hat{Q} = T \cdot Im \int dv\ \frac{mv^2}{2T}\hat{h} \tag{21}$$

using the normalized coefficient of $H \equiv -n(T/qB)(q\phi/T)^2 k_\theta$.

The electro-static gyro-kinetic equation[17] is given as

$$(\omega - \omega_d - \omega_{//} + iv_f)\, h = \frac{q}{T} F\,(\omega - \omega_*^T)\, J_0(\gamma)\, \phi \tag{22}$$

where ω_d, $\omega_{//}$ and v_f represent the magnetic drift frequency, the parallel motion frequency defined by $\omega_{//} \equiv (v_{//}/Rq(r))(m - nq(r) - i\partial/\partial\theta)$ and the collision operator, respectively. $J_0(\gamma)$ represents the zeroth-order Bessel function with a variable of $\gamma \equiv v_\perp k_\perp/\Omega$. ω_*^T is defined by $\omega_*^T \equiv \omega_*\{1+\eta(E/T-3/2)\}$ and $\omega_* \equiv Tk_\theta/qBL_n$. So, the normalized non-adiabatic part is

$$\hat{h} = \frac{\omega - \omega_*^T}{\omega - \omega_d - \omega_{//} + iv_f}\hat{F}\, J_0(\gamma) \tag{23}$$

where $\hat{F} \equiv F/n$. Using the definition of the denominator as $d \equiv \omega - \omega_d - \omega_{//} + iv_f$, the imaginary part of $\hat{h}$ is

$$Im\ \hat{h} = \frac{\hat{F}\, J_0(\gamma)}{(Re\ d)^2 + (Im\ d)^2}\,(\gamma\, Re\ d - \omega_r\, Im\ d + \omega_*^T\, Im\ d) \tag{24}$$

Here, defining the two functions by

$$R_n \equiv \int dv \ \frac{\mathrm{Re}\ d}{(\mathrm{Re}\ d)^2 + (\mathrm{Im}\ d)^2} \hat{F} J_0(\gamma) \left(\frac{E}{T}\right)^n \tag{25}$$

$$I_n \equiv \int dv \ \frac{\mathrm{Im}\ d}{(\mathrm{Re}\ d)^2 + (\mathrm{Im}\ d)^2} \hat{F} J_0(\gamma) \left(\frac{E}{T}\right)^n \tag{26}$$

the normalized particle and heat fluxes of Eqs.(20) and (21) can be written as

$$\begin{pmatrix} \hat{\Gamma} \\ \hat{Q}/T \end{pmatrix} = \begin{pmatrix} I_0 & I_1 - \frac{3}{2} I_0 \\ I_1 & I_2 - \frac{3}{2} I_1 \end{pmatrix} \begin{pmatrix} \omega_* - \omega_r \\ \omega_* \eta \end{pmatrix} + \gamma \begin{pmatrix} R_0 \\ R_1 \end{pmatrix} \tag{27}$$

The heat flux subtracting the convective energy flux, q=Q-(3/2 or 5/2)TΓ[18], is

$$\begin{pmatrix} \hat{\Gamma} \\ \hat{q}/T \end{pmatrix} = \begin{pmatrix} I_0 & I_1 - \frac{3}{2} I_0 \\ I_1 - \frac{3//5}{2} I_0 & I_2 - \frac{3}{2} I_1 - \frac{3//5}{2} I_1 + \frac{3//5}{2} \frac{3}{2} I_0 \end{pmatrix} \begin{pmatrix} \omega_* - \omega_r \\ \omega_* \eta \end{pmatrix} + \gamma \begin{pmatrix} R_0 \\ R_1 - \frac{3//5}{2} R_0 \end{pmatrix} \tag{28}$$

where 3//5 represents 3 or 5. In the above equations, it can be considered that the terms with $\omega_* - \omega_r$ and $\omega_* \eta$ correspond to the density and temperature gradient terms, respectively (where we assumed that ω_r is proportional to ω_*). Here, we consider the case of $\omega_* >> \gamma$ and neglect the second term of right hand side in Eq.(28). In this case, the transport coefficients can be easily evaluated, and the condition of $\alpha<0$ corresponds to $I_1/I_0<3/2$ for the normal density and temperature profiles of $\eta>0$.

To clear the relations between the transport coefficients, we estimate the integral function, I_n. For an estimation of qualitative feature, an approximate velocity dependence of integrand is important rather than the detail of the functional structure. Therefore, approximating the velocity dependence as

$$\frac{\mathrm{Im}\ d}{(\mathrm{Re}\ d)^2 + (\mathrm{Im}\ d)^2} \equiv K V^N \tag{29}$$

where K is constant and $V \equiv v(m/2T)^{0.5}$, Eq.(26) can be written as

$$I_n = \frac{4}{\sqrt{\pi}} K \int dV \cdot V^{N+2n+2} \exp(-V^2) \tag{30}$$

where $\hat{F}=(m/2\pi T)^{3/2}\exp(-mv^2/2T)$ was used and the effect of finite larmor radius was neglected. Using the formulas of

$$\int_0^\infty dx \cdot x^{2n+1} \exp(-x^2) = \frac{1 \cdot 2 \cdot 3 \cdots (n-1) \cdot n}{2} \tag{31}$$

$$\int_0^\infty dx \cdot x^{2n} \exp(-x^2) = \frac{1 \cdot 3 \cdot 5 \cdots (2n-1)}{2^{n+1}} \sqrt{\pi} \tag{32}$$

the ratios of I_1/I_0 and I_2/I_0 was calculated. The results were fitted by exponential functions as $I_1/I_0 \approx 1.42 \times 10^{0.21N}$ and $I_2/I_0 \approx 3.35 \times 10^{0.29N}$ (as shown in Fig.4.

From Eq.(28),

$$\Gamma_k = -\omega_*^2 L_n^2 \left(\frac{q\phi}{T}\right)^2 \left\{ I_0 \, \Delta\hat{\omega} \frac{\partial n}{\partial r} + \left(I_1 - \frac{3}{2} I_0\right) \frac{n}{T} \frac{\partial T}{\partial r} \right\} \tag{33}$$

$$q_k = -\omega_*^2 L_n^2 \left(\frac{q\phi}{T}\right)^2 \left\{ n \left(I_1 - \frac{3//5}{2} I_0\right) \Delta\hat{\omega} \frac{T}{n} \frac{\partial n}{\partial r} + n \left(I_2 - \frac{3}{2} I_1 - \frac{3//5}{2} I_1 + \frac{3//5}{2} \frac{3}{2} I_0\right) \frac{\partial T}{\partial r} \right\} \tag{34}$$

where $\Delta\hat{\omega} \equiv (\omega_* - \omega_r)/\omega_*$ and its value is positive because $\omega_* > \omega_r$[19]. From Eqs.(33) and (34), the ratios of χ/D, α/D and β/D can be written as

$$\frac{\chi}{D} \Delta\hat{\omega} = \frac{I_2}{I_0} - \frac{6//8}{2} \frac{I_1}{I_0} + \frac{9//15}{4} \tag{35}$$

$$\frac{\alpha}{D} \frac{T}{n} \Delta\hat{\omega} = \frac{I_1}{I_0} - \frac{3}{2} \tag{36}$$

$$\frac{\beta_n}{DT} = \frac{I_1}{I_0} - \frac{3//5}{2} \qquad (37)$$

and the calculated results are shown in Fig.5.

Here, it should be noted that N corresponds to a measure of collisionality ; N>0 and N<0 correspond to collisional and collisionless regimes, respectively. This relation is easily understood by considering that the collision operator ν_f has a velocity dependence of v^{-3}. From the figure, $\alpha<0$ appears in a region of $N\leq 0$ (collisionless regime), which is consistent with the result of Terry[20]. χ/D is positive for any values of N. With respect to β, the relation of $\beta<-(T/n)D$ is satisfied in a collisionless regime (we found in Sec.II that the relation of $\chi_{PM}>\chi_{PB}$ corresponds to $\beta<-(T/n)D$). These calculated results are consistent with several experimental observations. The first is the coupling between density and heat pulse propagations. In large tokamaks such as JET and JT-60 (of which plasma parameters are in a collisionless regime), the density and heat pulses induced by the internal disruptions are not coupling (the both pulses propagate with different propagating speeds). On the contrary, it was observed in TEXT[6,7] (the plasma parameters are in a collisional regime[20]) that the both pulses are closely coupling and D_{PM} is larger than D_{PB} by a several factor. Compared with the calculated results, it can be considered that the close coupling of the two pulses is due to the effect from the off-diagonal particle flux of $\alpha>0$, which is contrary to the density decrease due to temperature perturbation found in large tokamaks[12,13], and that the particle diffusivity estimated from the perturbation method becomes close to χ rather than D in the case of $\alpha>0$. The second experimental observation is the discrepancy between χ_{PM} and χ_{PB}. From the experiments it was found that in small tokamaks[1,2] (in a collisional regime) $\chi_{PM}=\chi_{PB}$ and in large tokamaks[3,4] (in a collisionless regime) $\chi_{PM}>\chi_{PB}$. These observations are consistent with the calculated result that the relation of $\beta<-(T/n)D$ is satisfied only in a collisionless regime.

In our approximate estimation of ExB convective fluxes, the transport coefficients were conducted using the assumptions : (1) $\omega_r>>\gamma$, (2) ω_r is proportional only to ω_* and (3) an approximate velocity dependence of Eq.(29). Therefore, in order to confirm the exact relation between ExB convective fluxes and off-diagonal flux terms, more accurate calculation is necessary.

V. CONCLUSION

As a conclusion, it is considered that the off-diagonal transport term is a plausible candidate, which explains the experimentally observed discrepancies between thermal and particle diffusivities estimated from the perturbation method and energy/particle balance analysis. Evidence of temperature gradient driven particle flux was observed from the sawtooth induced density propagation phenomenon in JT-60 and it was confirmed using the numerical simulation of the measured chord integrated electron density. However, up to now, no experimental observations can be obtained with respect to the off-diagonal heat flux. We estimated the transport coefficients of ExB convective fluxes using a quasi-linear transport formulation, and it was found that these fluxes are consistent with the several experimental observations. We consider that the further investigations for these problems are necessary in order to examine the influence of off-diagonal transport terms on tokamak confinement.

ACKNOWLEDGEMENTS

The authers are grateful for many useful discussions with menbers of the JT-60 Team. In particular, we would like to thank Drs. A. Funahashi, M. Azumi and S. Konoshima.

REFERENCES

[1]M. Soler, J. D. Callen, Nucl. Fusion 19, 703 (1979)
[2]J. D. Bell, J. L. Dunlap, V. K. Pare, J. D. Callen, H. C. Howe, E. A. Lazarus, M. Murakami, C. E. Thomas, Nucl. Fusion 24, 997 (1984)
[3]E. D. Fredrickson, J. D. Callen, K. Mcguire, J. D. Bell, R. J. Colchin, P. C. Efthimion, K. W. Hill, R. Izzo, D. R. Mikkelson, D. A. Monticello, V. K. Pare, G. Taylor, M. Zarnstorff, Nucl. Fusion 26, 849 (1986)
[4]B. J. D. Tubbing, N. J. Lopes Cardozo, M. J. Van Der Wiel, Nucl. Fusion 27, 1843 (1987)
[5]G. J. Jahns, S. K. Wong, R. Prater, S. H. Lin, S. Ejima, GA Technologies Report GA-A17858 (1985)
[6]S. K. Kim, D. L. Brower, W. A. Peebles, N. C. Jr. Luhmann, Phys. Rev. Lett. 60, 577 (1988)
[7]D. L. Brower, S. K. Kim, K. W. Wenzel, M. E. Austin, M. S. Foster, R. F. Gandy, N. C. Jr. Luhmann, S. C. Mccool, M. Nagatsu, W. A. Peebles, Ch. P. Ritz, C. X. Yu, Phys. Rev. Lett. 65, 337 (1990)
[8]A. Gondhalekar, A. D. Cheetham, J. C. M. De Haas, A. Hubbard, J. O'rourke, M. L. Watkins, Plasma Phys. Controll. Fusion 31, 805 (1989)
[9]M. Hossain, M. Kress, P. N. Hu, A. A. Blank, H. Grad, Phys. Rev. Lett. 58, 487 (1987)
[10]K. W. Gentle, Phys. Fluids 31, 1105 (1988)
[11]C. M. Bishop, J. W. Conner, Plasma Physics and Controlled Fusion 32, 203 (1990)
[12]K. Nagashima, T. Fukuda, M. Kikuchi, T. Hirayama, T. Nishitani, H. Takeuchi, submitted to Nucl. Fusion
[13]G. M. D. Hogeweij, J. O'rourke, A. C. C. Sips, J. C. M. De Haas, Proc. 17th European Conf. on Contr. Fusion and Plasma Physics, Amsterdam 1990, Part I, p.158
[14]J. D. Callen, J. P. Christiansen, J. G. Cordey, P. R. Thomas, K. Thomsen, Nucl. Fusion 27, 1857 (1987)
[15]N. A. Krall, J. B. Mcbride, Nucl. Fusion 17, 713 (1977)
[16]R. E. Waltz, W. Pfeiffer, R. R. Dominguez, Nucl. Fusion 20, 43 (1980)

[17]W. M. Tang, Nucl. Fusion 18, 1089 (1978)
[18]D. F. Duchs, JET-R(89)13
[19]W. Horton, in Basic Plasma Physics II (A. A. Galeev, R. N. Sudan, Editors), North Holland 383(1984)
[20]P. W. Terry, Phys. Fluids B 1, 1932(1989)

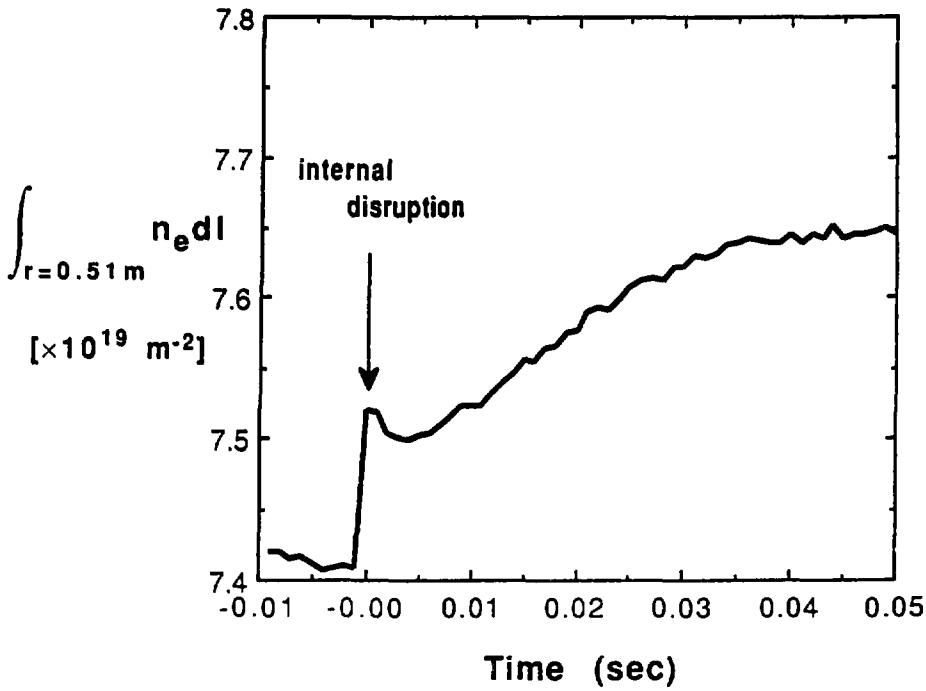

Fig. 1 Density pulse propagation induced by the internal disruption measured from FIR interferometer viewing the vertical chord at r=0.51 m.

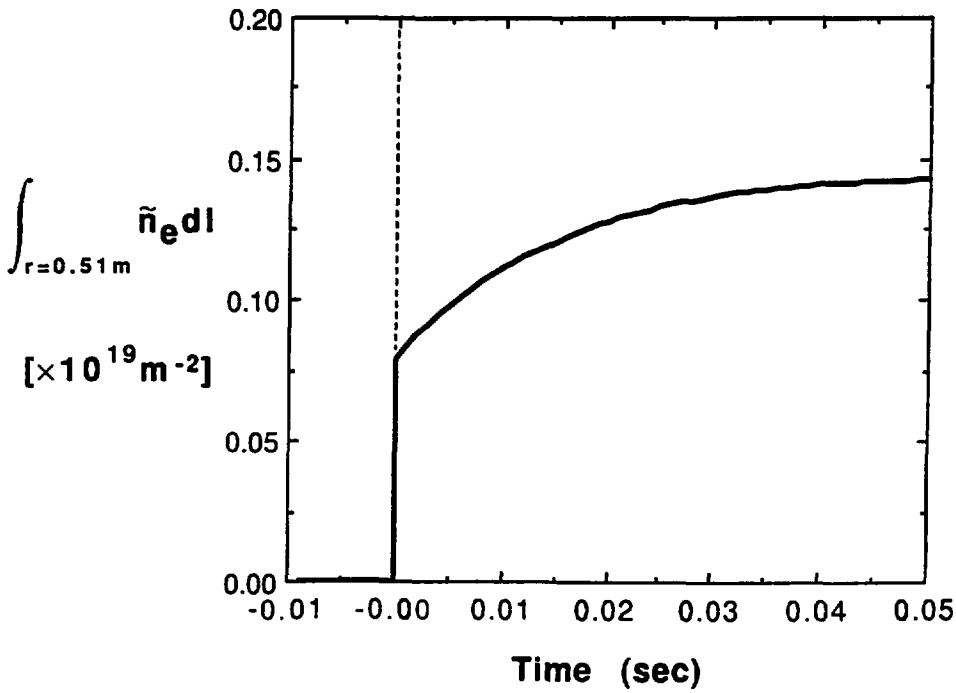

Fig. 2 Calculated chord-integrated density perturbation using Eq.(5) with the parameters of a_p=0.9 m, r_s=0.35 m, D=0.1 m^2/sec, α=0.0 $m^2/sec \cdot m^{-3}/keV$ and $n_0(r)=5.0(1-r^2)^{0.5}\times10^{19}$ m^{-3}. The initial perturbation profile was determined to be flat in the mixing radius.

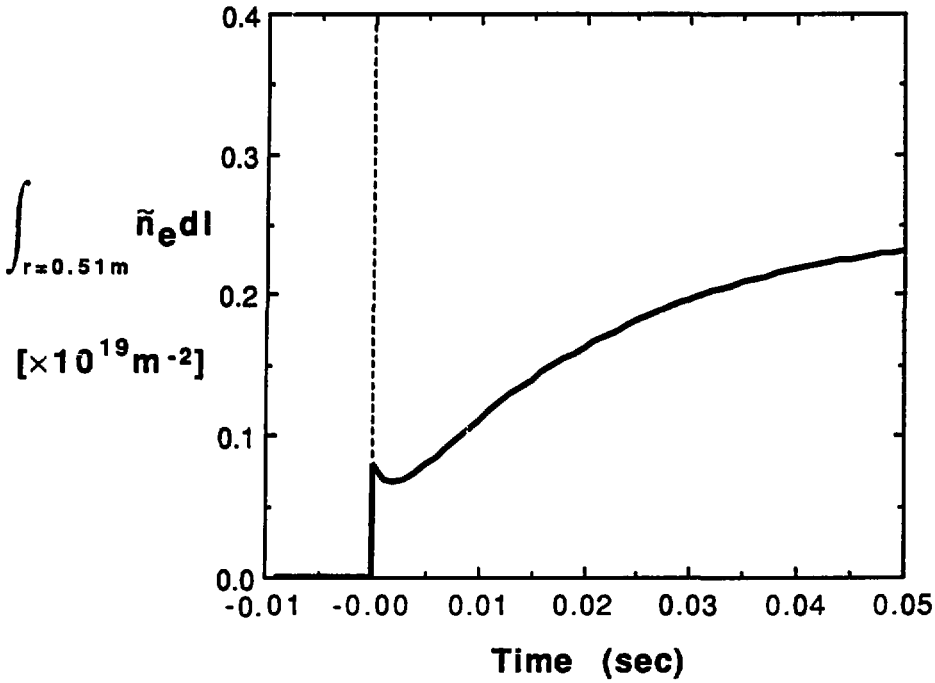

Fig. 3 Calculated chord-integrated density perturbation using Eqs.(5) and (6) including the off-diagonal terms with the parameters of a_p=0.9 m, r_s=0.35 m, D=0.25 m^2/sec, α=-0.3×10^{19} m^2/sec·m^{-3}/keV, χ=1.0 m^2/sec, β=-0.15×10^{-19} m^2/sec·keV/m^{-3}, $n_0(r)$=$5.0(1-r^2)^{0.5}\times10^{19}$ m^{-3}, $T_0(r)$=$4.0(1-r^2)^{1.5}$ keV. The initial perturbation profiles were determined to be flat in the mixing radius.

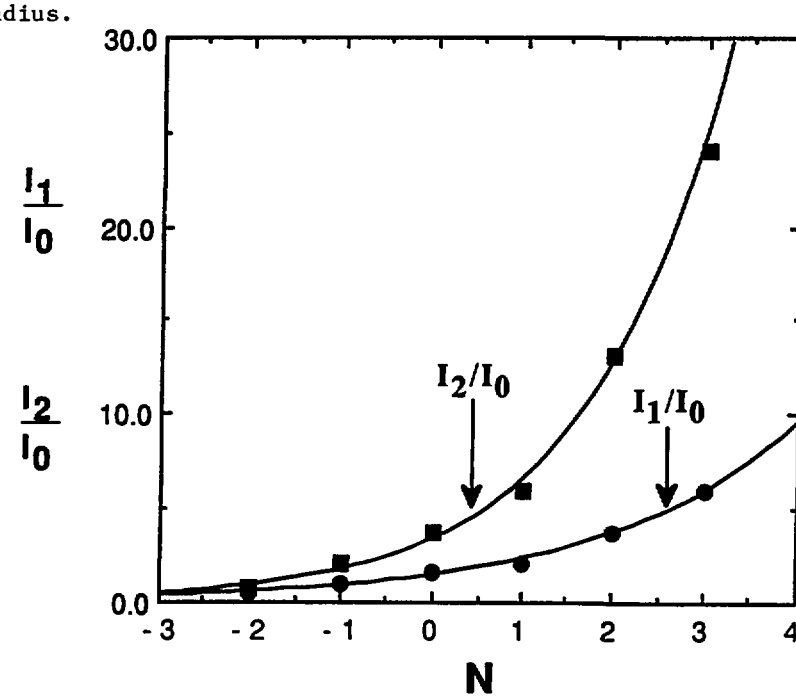

Fig. 4 The ratios of I_1/I_0 and I_2/I_0 as a function of N. Solid circle and solid square represent the points of I_1/I_0 and I_2/I_0 obtained from Eqs. (30) to (32), respectively. The fitting curves are I_1/I_0=$1.42\times10^{0.21N}$ and I_2/I_0=$3.35\times10^{0.29N}$.

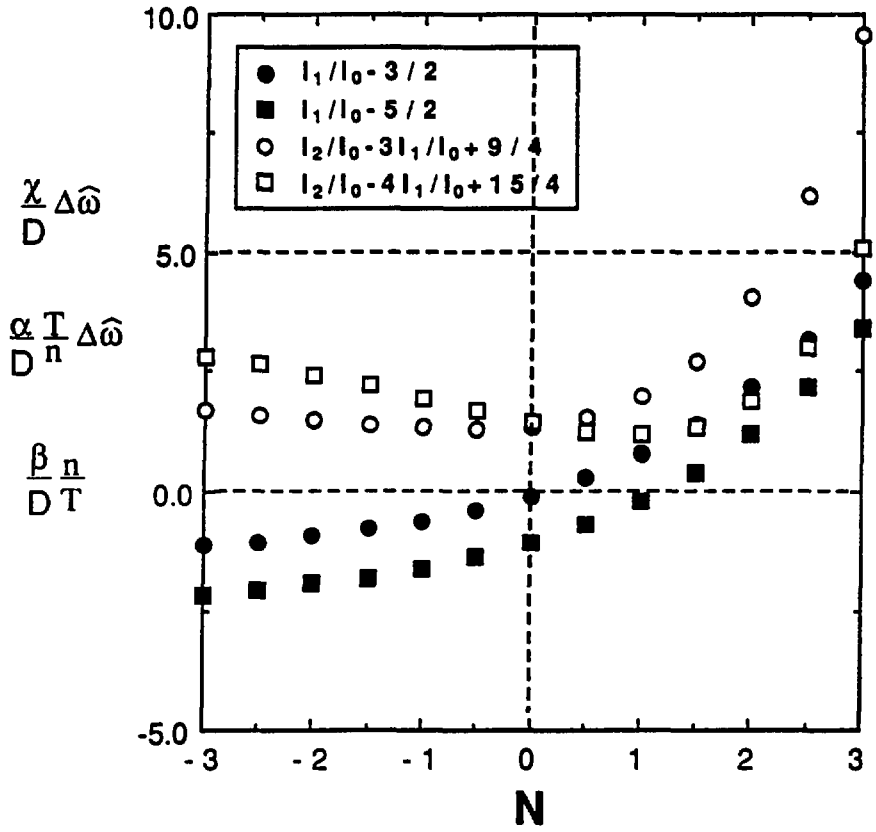

Fig. 5 The calculated values of $(\chi/D)\Delta\hat{\omega}$, $(\alpha/D)(T/n)\Delta\hat{\omega}$ and $(\beta/D)(n/T)$ as a function of N. Each symbols represent $I_1/I_0-3/2$(solid circle), $I_1/I_0-5/2$(solid square), $I_2/I_0-3I_1/I_0+9/4$(open circle) and $I_2/I_0-4I_1/I_0+15/4$(open square), respectively.